EFDA–JET–PR(14)26

P.T. Lang, H. Meyer, G. Birkenmeier, A. Burckhart, I.S. Carvalho, E. Delabie, L. Frassinetti, G. Huijsmans, G. Kocsis, A. Loarte, C.F. Maggi, M. Maraschek, B. Ploeckl, F. Rimini, F. Ryter, S. Saarelma, T. Szepesi, E. Wolfrum, ASDEX Upgrade Team and JET EFDA contributors

ELM Control at the L-H Transition Achieved by Pellet Pacing in the All-Metal Wall Tokamaks ASDEX Upgrade and JET

ELM Control at the L-H Transition Achieved by Pellet Pacing in the All-Metal Wall Tokamaks ASDEX Upgrade and JET

P.T. Lang[1], H. Meyer[2], G. Birkenmeier[1], A. Burckhart[1], I.S. Carvalho[3], E. Delabie[4], L. Frassinetti[5], G. Huijsmans[6], G. Kocsis[7], A. Loarte[6], C.F. Maggi[1], M. Maraschek[1], B. Ploeckl[1], F. Rimini[2], F. Ryter[1], S. Saarelma[3], T. Szepesi[7], E. Wolfrum[1], ASDEX Upgrade Team and JET EFDA contributors*

JET-EFDA, Culham Science Centre, OX14 3DB, Abingdon, UK

[1]MPI für Plasmaphysik, Boltzmannstr. 2, 85748 Garching, Germany
[2]Culham Centre for Fusion Energy, Culham Science Centre, Oxfordshire, OX14 3DB, UK
[3]Instituto de Plasmas e Fusão Nuclear, Instituto Superior Técnico, Universidade de Lisboa, P-1049-001 Lisboa, Portugal
[4]FOM-DIFFER, NL-3430 BE Nieuwegein, The Netherlands
[5]Royal Institute of Technology (KTH), Valhallavägen 79, 100 44 Stockholm, Sweden
[6]ITER Organization, Cadarache, F-13067 Saint-Paul-lez-Durance, France
[7]Wigner RCP, RMI, Konkoly Thege 29-33, H-1121 Budapest, Hungary
** See annex of F. Romanelli et al, "Overview of JET Results", (24th IAEA Fusion Energy Conference, San Diego, USA (2012)).*

Preprint of Paper to be submitted for publication in
Plasma Physics And Controlled Fusion

ABSTRACT

On ITER pellets are foreseen for ELM control and fuelling. More importantly ELM control in particular control of the first ELM needs to be demonstrated already in the non-nuclear phase of ITER during operation in H or He. Whilst D pellets have been established as ELM control technique in the stationary phase with D target plasmas in devices with C as plasma facing component, the question of other isotopes and non-stationary phases are less well known. Here, we report on new pellet triggering experiments in ASDEX Upgrade and JET mimicking specific ITER operating scenarios. Both machines are equipped with a full metal wall, where recent investigations have shown that pellet triggering and pacing become more intricate. On both machines ELM triggering by D pellets injected into D plasmas during extended ELM free phases, often following the L → H transition has been demonstrated. In both devices the pellets are found to induce ELMs under conditions far from the stability boundary for type-I ELMs. Furthermore, on ASDEX Upgrade this study was conducted during L → H transitions in the current ramp-up phase as foreseen for ITER. In addition, the pellet ELM trigger potential was proven at ASDEX Upgrade with a correct isotopic compilation for the non-nuclear phase on ITER, namely H pellets into either He or H plasmas. Results from this study are encouraging since they demonstrated the pellets potential to provoke ELMs even under conditions quite far from the stability boundaries attributed to the occurrence of spontaneous ELMs. However, with the change from C to an all-metal plasma facing components recently examples have been found on both machines where pellets failed to establish ELM control under conditions where this would be expected and needed. Consequently, a major task of future investigations in this field will be to shed more light on the underlying physics of pellet ELM triggering process, before sound predictions for ITER are possible.

INTRODUCTION

Operating ITER in the reference inductive scenario at the design values of $I_P = 15MA$ and $Q_{DT} = 10$ relies on good H-mode confinement facilitated by the presence of a strong edge transport barrier and a sufficiently high plasma pressure pedestal. The steep gradients evolving at the edge can drive MHD instabilities resulting in an Edge Localized Mode (ELM) producing rapid energy burst from the pedestal region. Without dedicated ELM control, the resulting transient heat loads on plasma facing materials in ITER become critical for operation at a plasma current $I_P \approx 9.5MA$ [1]; progressing to higher I_P would result in an intolerably short life time of the divertor plates [2]. Currently, there are several options considered for this inevitable ELM actuation, but all of them need further validation for the ITER tasks. Evidently, the main task in this context is to achieve sufficient mitigation of the peak power flux to the divertor in appropriate scenarios, either by suppression or mitigation of ELMs. ELM control requirements in ITER have recently received focussed attention [1] in relation with the proposal to start ITER operation with a Tungsten (W) divertor, which was originally foreseen for the beginning of nuclear operations (DD and DT plasmas) and is now planned also for the start of ITER operation in the non-nuclear phase (H and He plasmas) [3].

For the initial ITER operation the plasma current will be limited to $I_P \approx 7.5$MA and hence ELMs are not likely to cause unacceptable divertor erosion or melting. However, W will be produced in between and by the ELMs. Hence, a minimum ELM frequency may be required to maintain a sufficiently low W concentration in the main plasma [1]. Since ITER is expected to enter the H-mode already during the current ramp up phase, the mitigation technique must be compatible with a still changing plasma shape and edge magnetic configuration. Hence, for any considered control tool demonstration of successful actuation already immediately before and during the L to H transition is required. Crucial questions are whether the technique has an impact on the L → H transition power threshold and if there is a residual influence on the final steady-state H-mode.

Injection of solid pellets formed from frozen fuel has been demonstrated as a very well proven technique for the control of the ELM frequency in several tokamaks e.g. ASDEX Upgrade (AUG) [4], JET [5] and DIII-D [6]. Consequently, a suitable system is under development for controlled ELM triggering at ITER by injection of pellets carrying at least 2.0×10^{21} particles [1] from the torus outboard [7].

Here, we report on corresponding experiments conducted at AUG and JET. Employing pellet injection for ELM control at the L → H transition, they aim to mimic initial ITER conditions (H pellets in H/He plasma during I_P ramp). Although a full coverage of all aspects in a single demonstration experiment could not be achieved, all critical issues were covered one by one.

1. SET UP

Experiments reported have been performed in the two tokamaks AUG and JET, both operated with all-metal walls.

AUG is a medium-sized divertor tokamak (major radius $R_0 = 1.65$m, minor radius $a_0 = 0.5$m, I_P of up to 1.4MA, toroidal magnetic field B_t of up to 3.1T) with high shaping capability. It is equipped with a versatile set of auxiliary heating systems comprising 20MW neutral beam injection (NI), up to 6MW ion cyclotron resonance heating (ICRH) coupled power, and 5MW electron cyclotron resonance heating (ECRH). All plasma-facing components were converted stepwise from initially carbon (C) to W; complete W coverage has now been achieved. Details can be found in [8] and the references therein. Investigations reported here were all performed in the divertor IIc configuration, with a plasma volume of typically about 12m^3. Particle inventories of target plasma used in this study were in the order of 6×10^{20}D.

For investigations at ASDEX Upgrade the refurbished high speed launcher system based on a centrifuge accelerator and a looping transfer system is used. The system developed initially for fuelling purposes is capable of delivering pellets covering a wide size and speed range at repetition rates up to 80Hz from the torus inboard inclined by an angle of 72^o with respect to the horizontal mid plane [9]. For operation with D ice, reliable and persistent operation is achieved for the entire parameter regime. Experiments employing H pellets were essentially performed using large pellets at low to moderate speed. Since the cryostat system is mainly laid out for operation with D ice, the

lower triple point temperature of H compared to D resulted in a deficient cool down of the H ice rod. Hence, the lower yield strength of the pellets resulted in reduced delivery reliability, in particular too low for the task of ELM control when using small pellets. The pellet observation system was upgraded as well and it now allows fast individual pellet tracking. For the smallest possible pellet size the designated particle inventory is 1.5×10^{20}D, large pellets contain nominally 3.7×10^{20}D. Although a significant fraction of the pellet mass is lost during the transfer, the amount dependent on pellet size and speed, predominantly intended for a particle fuelling system, already increases the plasma density significantly with every single pellet. A continuous pellet train as applied for ELM control purposes impacts on the plasma even more, causing considerable alterations of the initial plasma parameters. Hence, the magnitude of the unavoidable fuelling by the pellet on AUG is always significant.

The world largest divertor tokamak JET ($R_0 = 2.96$m, $a_0 = 1.25$m, $I_P \leq 4.5$MA, $B_t \leq 3.8$T) is operated since 2012 with the ITER-Like Wall (ILW). This metallic wall replaced previous C plasma-facing components by a combination of beryllium (Be) in the main chamber and W in the divertor, the configuration foreseen for ITER. The design of the ILW components has taken into account plasma operation at high auxiliary power of up to 40MW (NBI 35MW and ICRF 5MW) for up to 20s [10]. Pellets at JET are produced by the high frequency pellet injector (HFPI), installed at the end of 2007 undergoing several modifications since then [11]. The HFPI system was designed to launch pellets from three different injection locations either for fuelling or for ELM pacing purposes. The pellet speed can be adjusted by the propellant gas pressure in the blower gun acceleration unit. Size and hence pellet mass can be fine-tuned by the pellet length. In addition, two different diameters can be chosen for the extruded ice rod. While a diameter of 4mm produces large pellets designed for core fuelling, small pellets 1.5mm in diameter have been adapted for the specific needs of the ELM control task. In operation it turned out reliable pellet delivery could only be achieved when launching the pellets from the torus outboard. While the full designated repetition rate of 15Hz was achieved for large pellets, for the small pacing size pellets only one of the two installed extruders works reliably up to 25Hz rather than the nominal 50Hz for pacing. A further revision is planned to start in late 2014 and finished by mid-2015. The aim is to optimize the system for inboard launch, restricting to this singly launch location but allowing operation with full performance with respect to variability and reliability.

Pacing size pellets as applied in this study have a designated particle inventory of 2.1×10^{20}D. However, with a plasma volume of typically about 80m^3 and target plasma particle inventories in the order of 24×10^{20}D, the fuelling impact of the pellets becomes almost marginal when pellet rates are restricted to reasonably low values.

2. FIRST DEMONSTRATION AT ASDEX UPGRADE

Pellet pacing through the L → H transition during the current ramp-up was tested on AUG initially with D pellets into a D plasma, and compared to a reference shot without pellets. During this phase

the plasma shape and q_{95} still evolve. The pellet controlled shot (Pulse Number: 26772, red traces) is shown together with the reference discharge (Pulse Number: 26610, blue traces) in figure 1. The reference discharge shows a delay of about 70ms between entering the H-mode and the first ELM in the absence of active ELM control. The L → H transition is facilitated by an early heating phase applying a single NI beam. For this scenario, the threshold power for H-mode access due to the ITPA threshold scaling [12] is about 2.0MW; however careful investigation showed this value is reduced by about 25% in AUG since operated with an all W wall [13]. Hence, with a loss power (absorbed heating power – dW/dt) of about 2.0MW the plasma is still in the vicinity of the threshold. Sustained injection of pellets all through the L → H transition eliminated the ELM-free phase. Pellets arriving a few ms before the transition clearly do not trigger ELM like events. Pellets reaching the plasma immediately after the transition do trigger ELMs despite an edge pedestal just starting to evolve but still far from its final magnitude. In particular, the first ELM is already triggered at a plasma energy level even below the regime spanned by the spontaneous ELM cycle (indicated by the grey bar in the box labelled "MHD stored energy").

Pellet actuation increased particle fuelling by gas puffing (8×10^{20} D/s in both discharges) by about 60%, resulting in an about 40% increased divertor density and an elevated line averaged density as displayed in figure 1; however this did not show a significant impact on the confinement finally reached. As well, pellet injection did not seem to have a major impact on the L → H transition or cause an almost prompt transition due to the changed edge parameters as e.g. reported from DIII-D [14] or MAST [15] although inboard pellet launch is regarded helpful for optimization of the L–H transition [15].

3. ISOTOPE ADAPTION: H PELLETS IN HE AND H PLASMAS

To match the ITER requirements for the initial phase experiments with a correct isotopic compilation were performed on AUG. The technically more challenging launch of H pellets into H and He plasma was demonstrated as well. For operational restrictions already mentioned, this is accompanied by a strong fuelling impact, even more pronounced than in the case shown in figure 1.

A plasma scenario similar to the one used in D (see figure 1) but with He as main ion species was developed, as shown in the left part of figure 2. Again early heating triggered the L → H transition already during the current ramp up. However, only a very short (less than 10ms) phase without ELMs was observed before a dithering H – mode evolved [16]. A pellet arriving in this phase caused an MHD event composed from a pure pellet component as observed for the previously injected pellet during the L – Mode, and the pure dithering signature. This can be concluded from the frequency distribution of the spectral power from a typical magnetic pick up coil. The spectral power of the signal trace marked by the red box is shown in the right part of figure 2. It includes both a pellet arriving yet in the L- and the dithering H-Phase (onset of pellet ablation marked by arrows) and several spontaneous dithering events. This overlay formation from the pure pellet and the pure ELM activity was identified as typical fingerprint of a triggered ELM by an extensive wavelet analysis [17].

Moreover, this behaviour was found for different ELM types in a separate study [18]. In this

study, it is shown that pellets generally do trigger ELMs that correspond to the naturally occurring ELMs, provided the pellets are sufficiently small not to alter the plasma regime.

E.g. in type-I ELMy discharges type-I ELMs are triggered, whereas in type-III ELMy discharges type-III ELMs are triggered. In particular pellets did not trigger ELMs in the QH-mode, which is characterized by the absence of ELMs but type-I ELMs in ELM-free phase [18]. In conclusion, these results at least confirm the trigger potential for H pellets in He discharges.

Due to the unfavourably high threshold power expected for H-mode access, operation with H is the less probable non-nuclear start up scenario for ITER [1]. However, with respect to pellet based ELM controlling it could be the favourable option since no dilution of the target plasma would take place. In order to cover this scenario as well, H pellet injection into a H target plasma was tested.

For this, a scenario with long lasting ELM-free phase of more than 200ms duration was developed. The L → H transition was initiated during the plasma current flat-top phase by the sudden application of pure EC wave heating into an initial Ohmic phase. Pellets were injected at a very low frequency of 5Hz to avoid a too drastic fuelling effect. Figure 3 displays the result. In its left part the reference phase without pellets and the long phase ELM-free following the L → H transition is shown. The right part of figure 3 presents data from the following shot repeated with identical discharge setting but pellets added (marked by the arrows) to the second last pane of the right panel. The strong fuelling impact of the pellets is clearly visible. But it is also obvious that the first pellet after the L → H transition triggers a single ELM already about 130ms after transition while spontaneous ELM activity sets in only after about 200ms just like in the reference case. No corresponding event is triggered by the pellet arriving prior to the L → H transition. Hence, under these circumstances pellet ELM triggering also is capable to truncate the initial ELM-free phase in an H plasma.

4. CONFIRMATION AT JET AND ELIMINATION OF THE FUELING IMPACT

The interpretation of all experiments performed at AUG is complicated by the unfavorable ratio of pellet to plasma particle content. Efforts to produce and launch sub mm size pellets were unproductive. Most probably due to the increasingly unfavourable surface/volume ratio and dwindling heat capacity of the tiny ice bodies, smaller pellets showed a rapid decrease of delivery efficiency as fragmentation and dissolving sets in. Hence, fuelling unavoidably caused by the pellets always results in a significant impact on plasma density in a tokamak of the AUG size. This situation clearly can be improved at JET when pellets of about the same size as the smallest reliable ones at AUG are injected. Due to the much larger plasma volume of JET, the total density build-up is now no longer perturbative.

Experiments reported here were embedded in studies of the L → H transitions investigating the power threshold dependence on the plasma shape [19]. This investigation also assessed the impact of fuelling method and location on the threshold value. Replacing the gas puff partially by pellets (again D pellets in D plasmas) showed that pellets do have higher fuelling efficiency but do not alter the transition parameters with respect to density and heating power [19]. The experiment

where a train of pacing size pellets was launched at a rate of 25Hz (JET Pulse Number: 84730) is shown in the left part of figure 4, the reference discharge with pure gas fuelling (JET Pulse Number: 84726) in the right part. Pellet injection resulted in ELM control after the L → H transition. Due to the moderate density rise per injected pellet a density evolution almost matching the gas fuelled reference discharge was obtained. This was demonstrated for a pulse type displaying a pronounced ELM-free phase just after the L → H transition with gas fuelling. In such a discharge, every single pellet arriving after the L → H transition enforced an ELM accordingly, thus avoiding the ELM-free phase observed in the reference case. Notably, the density evolution was predominantly influenced by the change of confinement rather than the pellet fuelling.

5. STABILITY ANALYSIS OF THE JET DEMONSTRATION CASE

Already our investigations at AUG show clearly that ELMs can be triggered under circumstances where no spontaneous ELMs seem to occur yet. This indicates the strong external perturbation created locally by the pellet ablation plasmoid hits the stability limit in the edge already before this happens driven by internal plasma perturbations (e.g. fluctuations). Clearly, this calls for a closer investigation of the situation. Hampered by the strong pellet fuelling impact significantly distorting the pedestal region with respect to the reference cases, obviously the AUG experiments are not especially well suited for such a detailed analysis. On the other hand, the JET experiment presented above provides good data for the stability analysis. The discharges, for example, show no pellet specific influence on the L → H transition power threshold P_{LH}. Evidently, as pellets do increase the plasma density this in turn elevates P_{LH} as predicted for these plasma parameters [12]. In addition, a detailed study showed divertor and SOL geometry can have a strong impact on P_{LH} [19]. Comparing the pellet fuelled discharges with the density scan performed by gas fuelling no difference in L → H threshold behaviour is observed [19]. Data with pellet fuelling align well with gas fuelled data in the same plasma configuration and any applied combination of these two fuelling methods resulted in the same P_{LH} value for the same resulting plasma density. Hence, data taken from both the pellet controlled case and the reference phase showing virtually identical edge profiles in order to achieve sufficient precision were considered appropriate for a plasma stability analysis.

Obtained electron density and temperature profiles, used for this stability analysis, are shown by the solid lines in figure 5. A fitting procedure modelled data by a modified hyperbolic tangent function quantifying the edge barrier properties by a set of pedestal parameters. The fitting procedure considers the instrument function effect [20]. Experimental data were taken from the high resolution Thomson scattering (HRTS) system optimised for a good resolution of the plasma edge. Several profiles covering about 200ms, recorded at a 20Hz framing rate were overlaid in order to allow for less uncertainty in the fit. Profiles are selected in the pre-ELM phase, in a time interval from 70% to 99% of the ELM cycle. Profiles taken immediately after an ELM have been deselected. As a cross-check, a comparison to the data taken by the electron cyclotron emission (ECE) diagnostics was made, confirming the HRTS temperature data. Within the uncertainty of the analysis, there is

no difference in the edge profiles of the reference (blue dots in figure 5) and the discharge where pellet trigger ELMs already immediately after the L → H transition.

Due to the absence of ELMs for the reference case the amount of data and hence the fit quality is somewhat higher, hence it was chosen for the stability analysis. Since it represents a case where the heating power was just slowly ramped up for a precise determination of P_{LH} and the pedestal just starts evolving, it was recognized as one of the lowest pressure gradients yet observed in JET H-mode plasmas. As a consequence, it is very stable against peeling-ballooning modes.

Hence, it can be concluded an ELM can be triggered by a strong local 3D perturbation already significantly before the pedestal is fully established reaching its linear stability limit, as predicted e.g. by the non-linear MHD code JOREK upgraded to include an appropriate description of the pellet ablation physics [21]. Simulations show pellet triggering of ELMs can be caused by the toroidally localized high edge pressure regions produced by the localized deposition of particles by the pellet and their reheating by the plasma [22]. Indeed, as can be seen in figure 1, every single pellet arriving in the plasma (indicated by the intense ablation radiation shown in the lowermost box) triggers immediately an ELM. Due to the pellet induced changes in the edge plasma, some additional fuelling-induced ELMs appear as well.

For the stability analysis (details of the method can be found in [23]) an equilibrium was created matching the actual plasma as closely as possible. The plasma equilibrium is reconstructed by using the fitted T_e and n_e profiles (assuming $T_i = T_e$) to calculate the bootstrap current self-consistently using the formula from [24]. Using the current and pressure profiles as well as the plasma shape from EFIT reconstruction, the plasma equilibrium is calculated using the fixed boundary equilibrium code HELENA [25]. The equilibrium of this operational point is then used as a basis for stability analysis with the ELITE code [26]. For operational points found stable against peeling–ballooning modes (criterion used for an unstable mode $\gamma/\gamma_A > 0.03$, where γ is the mode growth rate and γ_A the Alfven frequency) usually the equilibrium is perturbed by varying the pressure gradient and current density in the edge region until the adjacent stability boundary is hit. However, we were not able to find any stability boundary in the vicinity of the operational point. Hence, the operational point was just put for illustration into the stability diagram of a normal type-I ELMy case taken for comparison from the stability analysis data base most similar with respect to the plasma configuration [27]. The stability diagram of the comparable scenario together with the operational point from the reference discharge where pellets already proved capable to trigger an ELM is presented in figure 6. It is very clear that the plasma is very stable for modes usually associated with type-I ELM triggering. The local analysis of ideal $n = \infty$ ballooning modes found the entire pedestal pressure gradient at least a factor of 2 below the stability limit with no access to the 2nd stability region. Typical JET Type-I ELMy pedestals are either close to the $n = \infty$ ballooning stability limit or in the 2nd stability region [28]. The ELMs in these plasmas are likely to be triggered by a non-ideal process such as a resistive instability or, as suggested by Futatani et al. [21] evolving from ballooning modes destabilized by the large 3D local pressure gradients of the pressure perturbation due to the pellet ablation.

6. CONCLUSION AND OUTLOOK

The study presented shows control of the ELM frequency by pellet pacing can be established while the plasma undergoes the L → H transition. Even all aspects of an application during the initial operational phase of ITER were demonstrated one by one. It is interesting how easy pellets can trigger ELMs although the edge is still far from the peeling-ballooning stability boundary. This becomes obvious already from the examples presented from AUG and was confirmed by a detailed analysis of the JET demonstration case. The question arises for the underlying physics to explain on the one hand the easiness of ELM control close to the L → H transition presented here and on the other hand the more intricate behaviour of pellet pacing in the stationary phase that has been also found in both devices when changing from C to all metal plasma facing components [29].

At JET after the installation of the ILW it was found sometimes pellets do not trigger ELMs under ELMy H-mode conditions where reliable triggering was found when operating with a C wall. Pacing and triggering attempts under steady state plasma conditions emerged a trigger lag time, i.e. a distinct period of time after a previous spontaneous or triggered ELM where a pellet fails to trigger an ELM while it succeeds afterwards [30]. For the better reliability and wide operational parameter range of the pellet system, investigations on this topic were repeated and refined at AUG. The presence of a trigger lag time in the all-metal wall device in contrast to behaviour found with at least partial C coverage of plasma facing components was clearly confirmed. Furthermore, at AUG it turned out the lag time does not significantly depend on pellet parameters size and speed but decisively on the plasma scenario [31]. In different plasma scenario, cases showing quite a variation with respect to their response on pellet triggering attempts were observed; two extreme examples are displayed in figure 7. Little trigger potential was found for the ITER base line scenario [32], discharges prone to impurity accumulation eventually finally causing fatal radiative losses due to a spontaneous ELM rate dropping too low. Several attempts to avoid this by establishing pellet ELM pacing essentially turned out not successful as pellets too often failed in triggering. A typical example is shown in the lower part of figure 7; arriving 89ms after the previous spontaneous ELM and thus already very late in the initial ELM cycle and the plasma almost fully recovered after the ELM crash, this pellet does not initiate an ELM. An opposed example can be seen in the upper part of figure 7. It represents a scenario with high auxiliary heating power applied resulting in a high plasma energy contend. In order to protect the divertor by radiative cooling, Nitrogen seeding was applied [33]. In general, under such plasma conditions a very high pellet ELM trigger potential is found. Again, a typical case is presented showing a triggering pellet arriving just 1.9ms after the onset of the previous spontaneous ELM although the plasma had just started to recover from the ELM crash. Reported results on ELM control under conditions mimicking the first application in ITER are quite encouraging, especially due to the fact our findings for AUG and JET operated with all-metal walls do agree so well.

Obviously, pellet ELM triggering is possible with the plasma edge far from its intrinsic stability

boundary. However, severe counterexamples were observed as well. This strongly indicates further attention must be devoted to this topic. A better understanding of the underlying physics of pellet ELM triggering is indispensable for providing reliable prediction for ITER, i.e. under which conditions pellet ELM control can be established. In particular, it would be beneficial to optimize the operational parameters of the pellet pacing system, namely pellet size, speed and launch position. As it is expected pacing pellets could carry already 40% of the particle flux required for pellet particle fuelling in ITER [1], a significant reduction of this flux would ease operation by disentangling the two crucial control parameters ELM frequency and plasma density. Furthermore, the impact of the pacing on the more crucial peak heat flux on the divertor has to be investigated. While DIII-D reports a reduction in proportion of at least the ELM frequency enhancement [6], JET and AUG found and virtually no reduction [31].

Experiments ongoing both on AUG and JET now aim to clarify the role of different plasma and pellet parameters in the triggering process. For example, Nitrogen seems to play a crucial role obviously fostering the pellet ELM triggering potential once its concentration reaches a sufficiently high level. As well, the poloidal location of the pellet perturbation has shown strong influence on the pellet trigger potential. Results from JET [34] show inboard pellets can trigger more easily than pellet arriving at the plasma magnetic low field side, and very recently as well indications for a pellet mass threshold for triggering were found. In addition, attempts are under way to create well documented cases with relevant plasma scenarios experimentally found close to both sides of the stability limit for pellet ELM triggering. Such data sets will provide instructive examples for detailed and more sophisticated modelling attempts.

ACKNOWLEDGMENTS

This work was supported by EURATOM and carried out within the framework of the European Fusion Development Agreement. The views and opinions expressed herein do not necessarily reflect those of the European Commission.

REFERENCES

[1]. A. Loarte et al., Nuclear Fusion **54** (2014) 033007
[2]. G. Federici et al., Plasma Physics and Controlled Fusion **45** (2003) 1523
[3]. D.J. Campbell et al., in Fusion Energy 2012 (Proc.24th Int. Conf. San Diego) [ITR/P1-18]. http://www-naweb.iaea.org/napc/physics/FEC/FEC2012/index.htm
[4]. P.T. Lang et al., Nuclear Fusion **44** (2004) 665
[5]. P.T. Lang et al., Nuclear Fusion **51** (2011) 033010
[6]. L.R. Baylor et al., Physical Review Letters **110** (2013) 245001
[7]. S. Maruyama et al, in Fusion Energy 2012 (Proc.24th Int. Conf. San Diego) [ITR/P5-24].
[8]. U. Stroth et al., 2013, Nuclear Fusion **53**, 104003
[9]. B. Plöckl and P.T. Lang, Review of Scientific Instruments **84** (2013) 103509

[10]. F. Romanelli and JET EFDA Contributors, 2013, Nuclear Fusion **53** 104002
http://iopscience.iop.org/0029-5515/53/10/104002/article
[11]. A. Geraud et al., 27th SOFT conference, Liège (Belgium) September 2012, P1.31.
http://sciconf.org/soft2012/ip/topic/c/session/p1/paper/31
[12]. Y.R. Martin.et al., 2008, Journal of Physics:Conference Series 123, 012033.
[13]. F. Ryter et al., 2013, Nuclear Fusion **53**, 113003
[14]. P. Gohil et al., 2001, Physical Review Letters **86**, 644
[15]. M. Valovic et al., 2012, Nuclear Fusion **52**, 114022
[16]. H. Zohm, Physical Review Letters **72** (1994) 222
[17]. F.M. Poli et al., 2010, Nuclear Fusion **50**, 025004
[18]. P.T. Lang et al., 2008, Nuclear Fusion **48**, 095007
[19]. H. Meyer et al., Proc.41th EPS Conf. Berlin 2014, P1.013
[20]. L. Frassinetti, 2012, Review of Scientific Instruments **83**, 013506
[21]. S. Futatani et al., 2014, Nuclear Fusion **54**, 073008.
[22]. G.T.A. Huysmans et al., 2009 Plasma Physics and Controlled Fusion **51**, 124012
http://iopscience.iop.org/0029-5515/53/12/123023/refs/9/article
[23]. S. Saarelma et al., 2009, Plasma Physics and Controlled Fusion **51**, 035001
[24]. O. Sauter, C. Angioni C and Y.R. Lin-Liu, Physics of Plasmas **6**, 2834 (1999).
[25]. G.T.A. Huysmans, J.P. Goedbloed, W.O.K. Kerner, Computational Physics (Proc. Int. Conf. Amsterdam, 1991),World Scientific Publishing, Singapore, 371 (1991).
[26]. H.R. Wilson, P.B. Snyder, G.T.A. Huysmans and R.L. Miller, Physics of Plasmas **9**, 1277 (2002).
[27]. M.N.A. Beurskens et al., 2013, Plasma Physics and Controlled Fusion **55** 124043
[28]. S. Saarelma et al. Nuclear Fusion **53**, 123012
[29]. P.T. Lang et al., Proc.40th EPS Conf. Espoo 2013, O2.102
[30]. P.T. Lang et al., 2013, Nuclear Fusion **53**, 073010
[31]. P.T. Lang et al., 2014, Nuclear Fusion **54**, 083009
[32]. J. Schweinzer et al., Proc.40th EPS Conf. Espoo 2013, P2.134
[33]. A. Kallenbach et al., 2012, Nuclear Fusion **52** 122003 doi:10.1088/0029-5515/52/12/122003
[34]. D. Frigione et al., Proc. 21st PSI Kanazawa 2014, P2.028

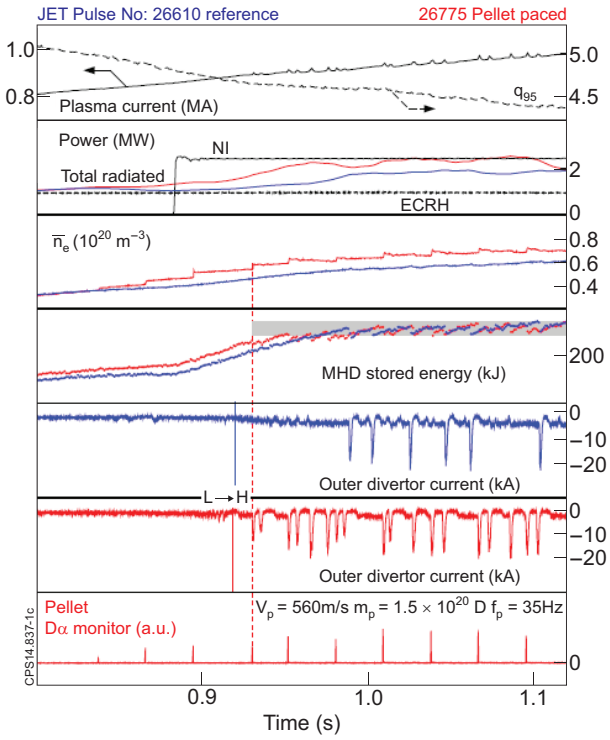

Figure 1: Demonstration of ELM control by pellet pacing at ASDEX Upgrade while the plasma undergoes the L → H transition during current ramp up with changing shape. The reference discharge (Pulse Number: 26610, blue traces) shows a delay of about 70ms between entering the H-mode and the first ELM in the absence of active ELM control. Sustained pellet pacing (Pulse Number: 26772, red traces) enforces ELM activity already virtually immediately after the L → H transition. Every pellet triggers an ELM but fuelling induced ELMs appear as well. The first ELM is triggered at a plasma energy level even below the regime spanned by the spontaneous ELM cycle (indicated by grey bar in box labelled "MHD stored energy").

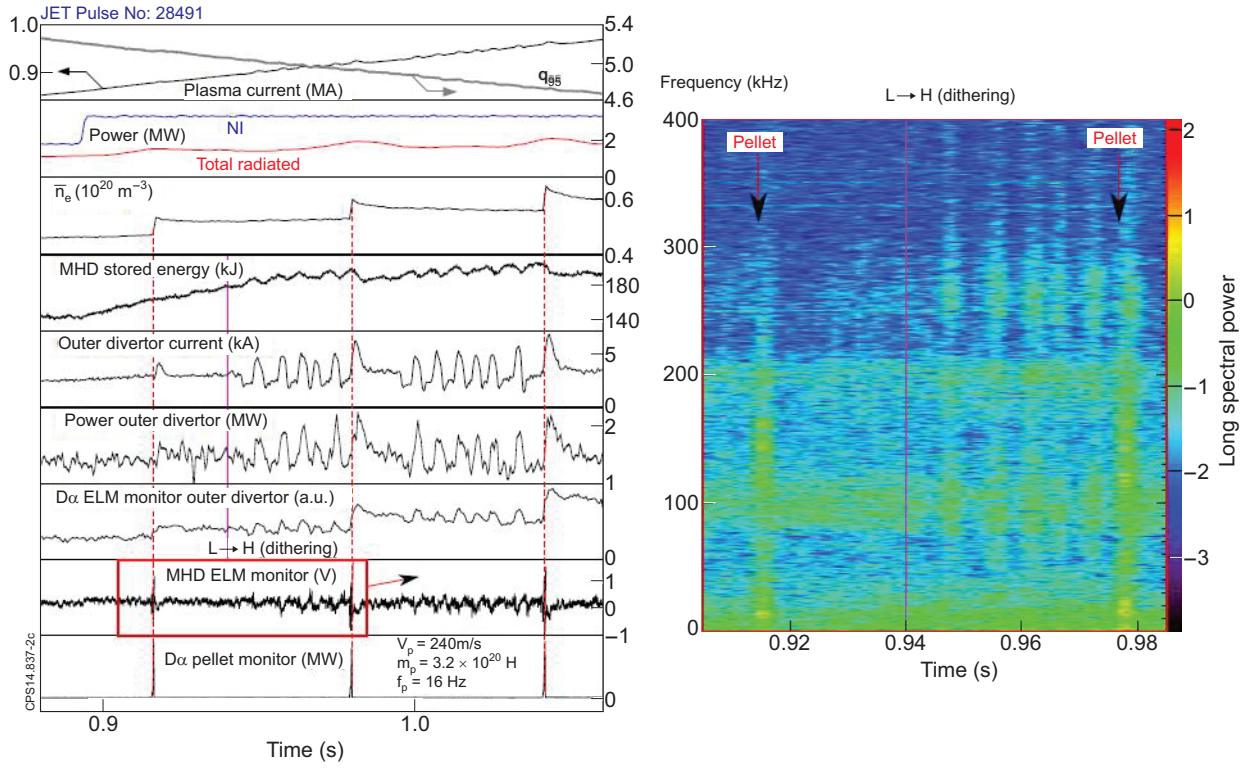

Figure 2: Demonstration of the pellet ELM trigger potential at ASDEX Upgrade for H pellets injected into a He plasma while the plasma undergoes the L → H transition during current ramp up with still changing shape. The L → H transition is followed here by a dithering ELM phase, pellets arrive both before and after the transition (left part). Analysis of the MHD activity recorded by a close by pick up coil (right part, according signal marked by red box in left part) shows the pellet arriving during the dithering phase triggers an event displaying a signature alike the superposition of a pure pellet (as measured during the L-mode) and a spontaneous ELM – as expected for a triggered ELM.

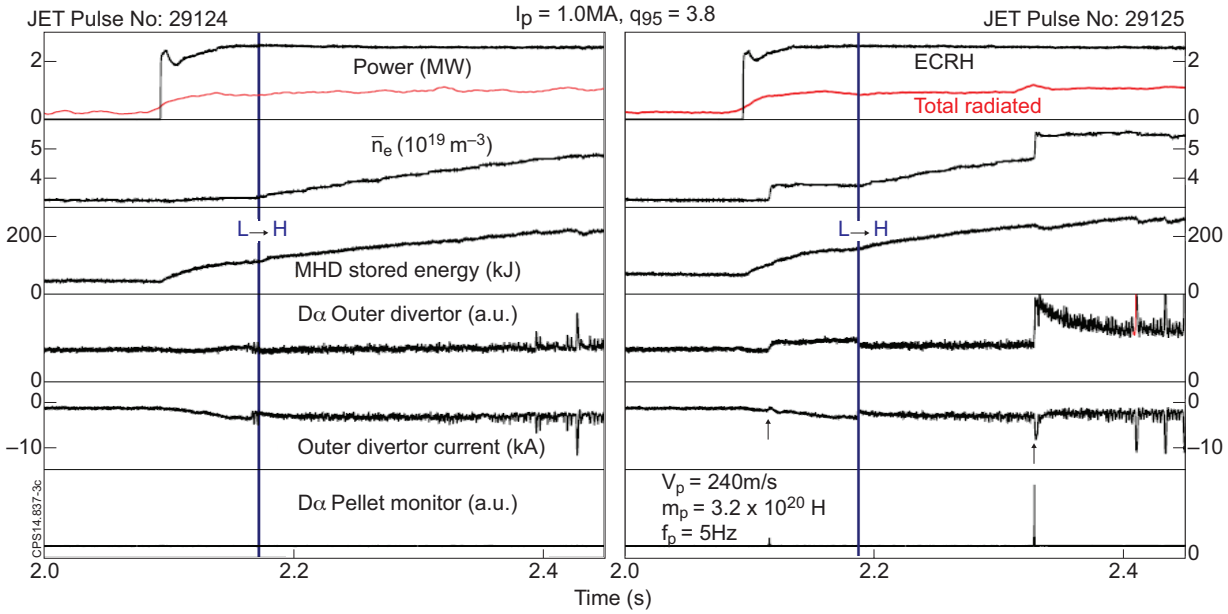

Figure 3: Demonstration of the pellet ELM trigger potential at ASDEX Upgrade for H pellets injected into a H plasma. A 200ms long ELM-free phase is initiated by EC heating applied to the initial OH current flat top plasma scenario in the reference phase (left). Low frequent pellets (5Hz, marked by the arrows) still cause significant fuelling; nevertheless spontaneous ELMs set in again after about 200ms like in the reference case. The first pellet arriving after the L → H transition triggers an ELM while no corresponding event is caused by the previous pellet.

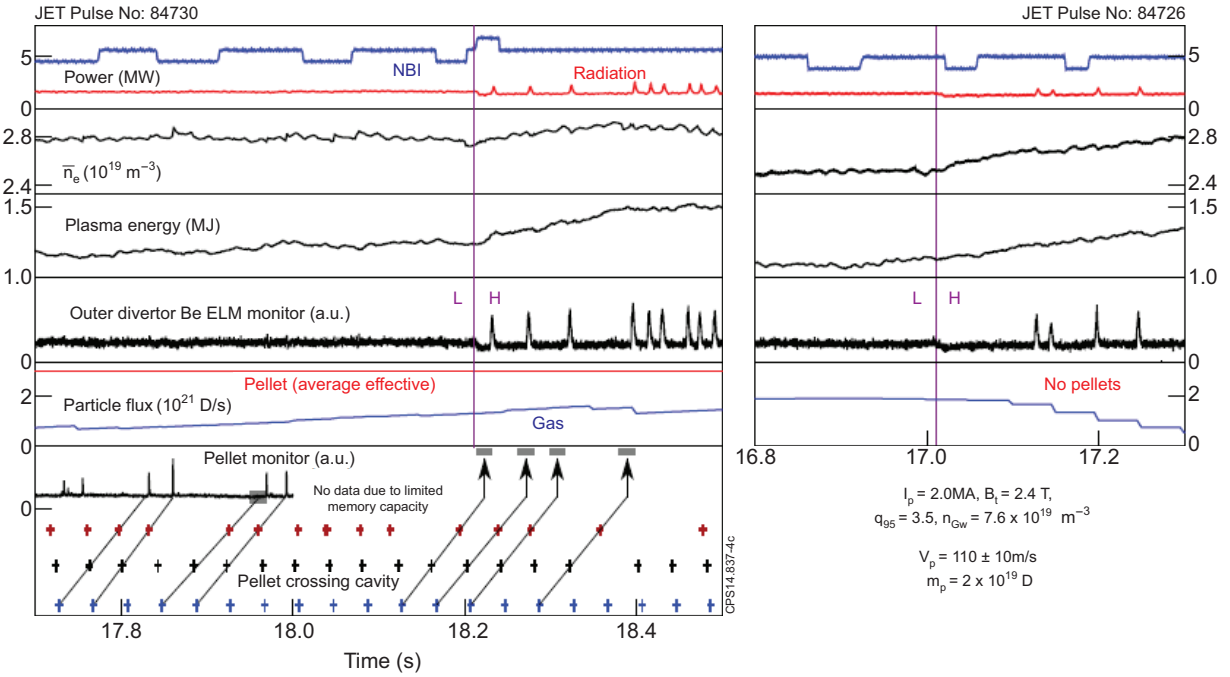

Figure 4: Demonstration of ELM control at JET by pellet pacing while the plasma undergoes the L → H transition. The reference discharge (JET Pulse Number: 84726, right) with pure gas fuelling shows a delay of about 110ms between entering the H-mode and the first ELM. Applying partial pellet fuelling (JET Pulse Number: 84730, left) results in a slightly higher density in the L-Mode phase due to better fuelling efficiency. In the H-mode phase a similar fuelling efficiency as in the gas reference is found but now every pellet triggers an ELM and the ELM-free phase is avoided. The first ELM is triggered in a still almost L-Mode like pedestal. Due to the higher density in the pellet case, the L → H transition occurs later and the pre-set timed pellet monitor run out of data memory. Pellet arrival in the plasma is estimated (uncertainty represented by the grey bars) from a time-of-flight analysis of the pellets passing through several cavities installed along the flight tubes, as shown in the lower box. Note the speed scatter resulting in a distorted pellet train frequency and the gap due to a pellet obviously destroyed in flight.

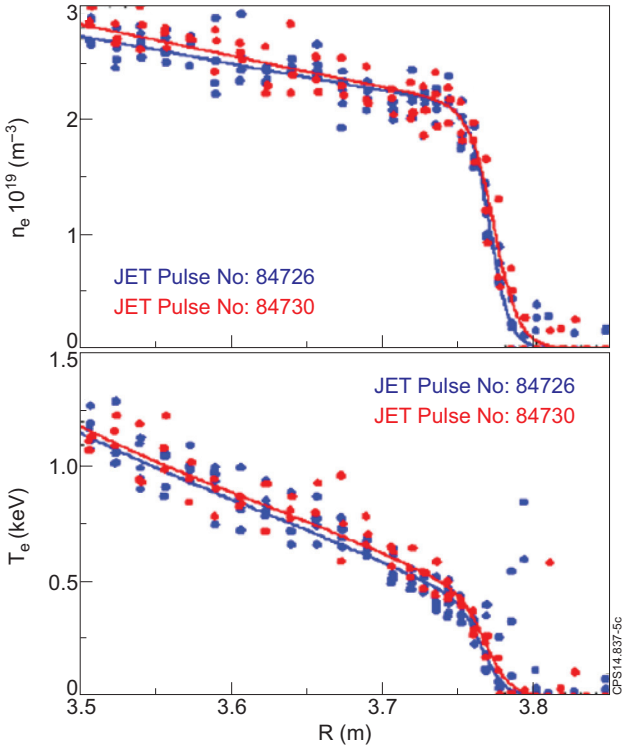

Figure 5: Edge density (upper box) and temperature profiles (lower box) as obtained by overlaying several profiles measured by the HRTS system from the phase following the L → H transition, deselecting profiles after an ELM crash. No significant differences are found for the reference (blue) and the case with pellet triggered early ELMs (red). Solid lines represent fits used for the stability analysis.

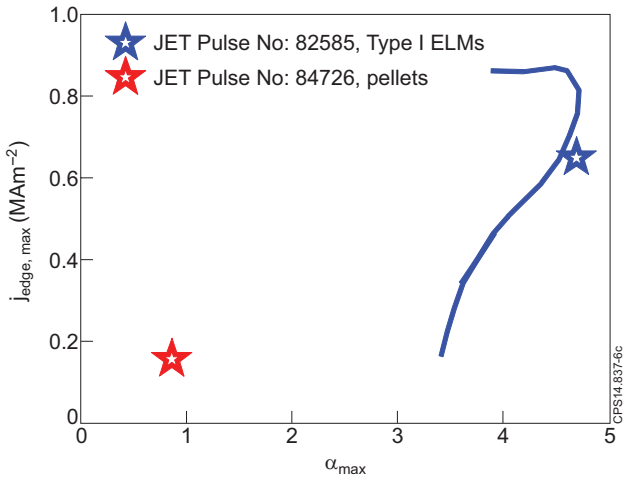

Figure 6: Edge stability diagram of a similar comparison discharge showing type-I ELMs at an operational point (blue star) close to the calculated peeling–ballooning stability (solid blue line). The operational point of the analysed reference discharge displaying an ELM-free phase but proved unstable against pellet triggering of ELMs (red star) is found quite afar from the stability boundary.

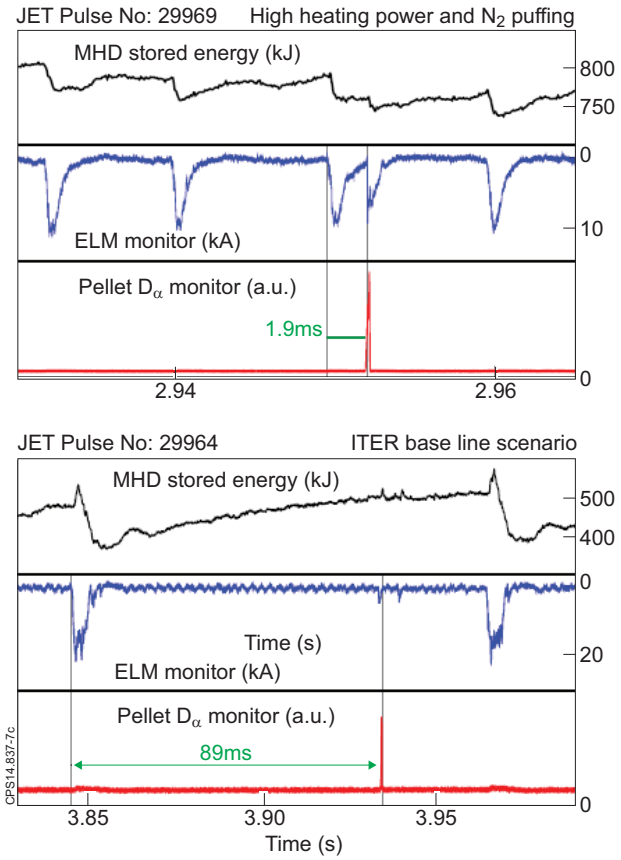

Figure 7: Most extreme cases observed for triggering lag times in AUG. Rather easy triggering is observed in plasmas with strong auxiliary heating and high confined energy. In such discharges, Nitrogen seeding had to be applied to provide divertor cooling. The example shows (upper box) a pellet arriving after only 1.9ms in the ELM cycle clearly triggering. In contrast, within the ITER baseline scenario suffering from low spontaneous ELM rates and becoming prone to impurity accumulation, attempts to enforce sufficient ELM activity fails. For the shown example, a pellet arriving 89ms after the start of the previous ELM does not succeed in triggering (lower box).